

Compact Long-Period Fiber Gratings With Resonance at Second-Order Diffraction

Jing-Chun Guo, Yong-Sen Yu, Xu-Lin Zhang, Chao Chen, Rui Yang, Chuang Wang, Rui-Zhu Yang, Qi-Dai Chen, and Hong-Bo Sun, *Member, IEEE*

Abstract—Compact 5-mm-long 100- μm -period long-period fiber gratings (LPGs) are fabricated by femtosecond laser direct writing. Nearly symmetrical photomodified grating segments located at the center of a fiber core lead to well-defined transmission spectra. The LPGs can couple the guided mode to high-order cladding modes of second-order diffraction, resulting in a high refractive index (RI) sensitivity of 5265 nm/RI units in the RI range of 1.433 \sim 1.443 and a low-temperature sensitivity of $-15.52 \text{ pm}/^\circ\text{C}$ from 20 $^\circ\text{C}$ to 500 $^\circ\text{C}$. The latter property is desired for crosstalk-free high-sensitivity RI sensors.

Index Terms—Femtosecond laser, fiber sensor, long-period fiber gratings (LPGs), second-order diffraction.

I. INTRODUCTION

LONG-PERIOD fiber gratings (LPGs) have been widely applied in telecommunications and optical sensing fields [1]–[3]. In comparison with general fiber Bragg gratings (FBGs), the LPGs possess higher sensitivity to the variation of refractive index (RI) because the evanescent field extends out of the fiber cladding as a result of core-cladding mode coupling [4]–[6]. LPGs are therefore considered as an ideal type of optical sensing architecture [2], [4]. However, the intrinsic shortcomings associated with the LPGs fabrication hinder their practical applications. Firstly, the length of the grating-bearing region of LPGs is too long, generally of the order of centimeters, to be incorporated into compact integrated systems. This comes from the relatively weak RI modulation ($\Delta n/n < 0.1\%$) in the mechanism of ultraviolet (UV) exposure and color center production in Ge-doped fibers. Secondly, the gratings tend to be degraded at a high temperature due to the thermal bleaching of the photorefractive structures. The degradation of the UV-light-induced index change was observed even at 85 $^\circ$ [7].

The femtosecond laser has been proved effectively to induce significant RI change in transparent solids by direct breaking of covalent bonds [8] or in liquid media by photopolymerization [9]. In the former case, a much larger $\Delta n/n$, from 0.1% to 1%, can be obtained and kept stable until the temperature is

high enough to soften or sublimate the matrix materials. The unique performance allows for not only a high-temperature working condition of fiber-grating sensors, but also a pronounced reduction of the grating length due to the sufficiently high RI modulation when the femtosecond laser is utilized for grating recording. Grating fabrication has actually been demonstrated by direct laser writing [10], exposure through phase mask [11], or interference ablation [12]. Different from FBGs, the fabrication of LPGs with irregular index modulation has not been achieved by infrared femtosecond laser direct writing to obtain ideal spectral performance [10]. This letter reports on the achievement of symmetrical photomodified segments that possess smaller diameter ($\sim 2 \mu\text{m}$) than that of the fiber core (8.5 μm) by femtosecond laser direct writing technique. The index change is found to occur exactly inside the fiber core. This, together with a utilization of the high-order propagating modes from HE_{1,22} to HE_{1,25} that are resonant at the second-order diffraction, leads to highly sensitive fine spectral feature in a compact 100- μm -period LPG.

II. EXPERIMENTS

Direct writing of LPGs in standard single-mode fibers (Corning SMF-28) with infrared femtosecond laser pulses was conducted with a Ti:sapphire regenerative amplifier laser system (Spectra Physics) operating at 800 nm. The pulse duration and the repetition rate were 100 fs and 1 kHz, respectively. The laser beam was focused into the fiber core via an oil-immersed 60 \times Olympus objective (N.A., 1.42). The diameter of the focal point was estimated to be 0.68 μm . The energy of the laser beam was adjusted by a neutral density filter. The fiber was mounted on a computer-controlled three-axis translation stage with a motion spatial resolution of 20 nm. The transmission spectral change of the LPG was monitored during the fabrication process by a broadband light source (Superk Compact, NKT Photonics) and an optical spectrum analyzer (OSA) (AQ6370B, Yokogawa) with a resolution of 0.1 nm.

Fig. 1(a) shows the side-view microscopic image of a typical LPG with 100- μm period and a duty cycle of 0.5. The number of periods is 50, indicating the total length of the grating-bearing region is only 5 mm. The cross-section microscope image shows that the index modulation is exactly located at the center of the fiber core as shown in Fig. 1(b). Well-defined photomodified segments with approximately 2- μm diameter are located at the center of the fiber core. No damage to the

Manuscript received March 17, 2012; revised June 2, 2012; accepted June 6, 2012. Date of publication June 11, 2012; date of current version July 20, 2012. This work was supported in part by the National Natural Science Foundation of China under Grant 90923037 and Grant 91123027.

The authors are with the State Key Laboratory on Integrated Optoelectronics, College of Electronic Science and Engineering, Jilin University, Changchun 130012, China (e-mail: yuys@jlu.edu.cn; hbsun@jlu.edu.cn).

Color versions of one or more of the figures in this letter are available online at <http://ieeexplore.ieee.org>.

Digital Object Identifier 10.1109/LPT.2012.2204243

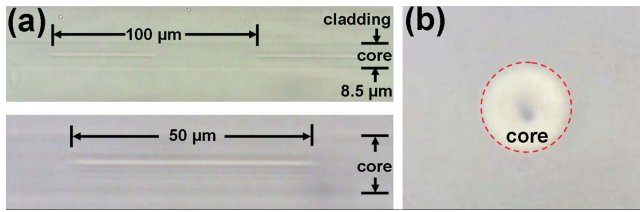


Fig. 1. (a) Side-view microscope image of RI modulation region in the fiber core. (b) Cross-section microscope image of RI modulation region in the fiber core.

cladding is observed. The experimental transmission spectrum exhibits good performance, as confirmed by Fig. 2(d), where four evident loss peaks from 1100 nm to 1700 nm appear. They are naturally ascribed to the coupling between the guided mode and the forward-propagating cladding modes [13]. The excess 4-dB loss is attributed to the light scattering from the structural damage induced by femtosecond laser inscription in the fiber core [10].

III. THEORETICAL MODELING

The coupling between the guided mode and the cladding modes of high diffraction orders was first reported by Shu et al. [14].

The phase-matching condition is written as

$$\lambda_{res} = (n_{co}^{eff} - n_{cl,m}^{eff})\Lambda/N \quad (1)$$

where λ_{res} is the resonant wavelength, Λ is the grating period, N is the diffraction order, and n_{co}^{eff} and $n_{cl,m}^{eff}$ are the effective indices of the guided mode and the m th cladding mode, respectively. This theory is in good agreement with the experimental results of ultra-long-period fiber gratings, and the coupling at high diffraction orders occurred to low-order cladding modes [14]. However, there is no report about the coupling between the guided mode and the high-order cladding modes of high diffraction orders. This letter reports on the coupling of the guided mode to the high-order cladding modes from HE1,22 to HE1,25 at the second-order diffraction.

Fig. 2(a) shows the relationship of the calculated resonant wavelength and the grating period for the coupling of the guided mode to the high-order cladding modes from HE1,15 to HE1,25 (the EH modes are not shown here because of the degeneration of high-order HE and EH modes). It was earlier reported that the coupling between the lower-order even cladding modes (below 40) and the guided mode is very weak, but for the high-order even cladding modes (above 40), the coupling strength is of the same magnitude compared with the odd modes [13]. The coupling constants of different high-order cladding modes are shown in Fig. 2(b), in which it is very clear that both the even and the odd modes exhibit comparable coupling strengths. The coupling of the HE1,15 and HE1,16 modes to the guided mode corresponds to the first-order diffraction resonances of the 100- μ m period grating and the coupling of the cladding modes from HE1,22 to HE1,25 to the guided mode corresponds to the second-order diffraction resonances of the 50- μ m period grating. However,

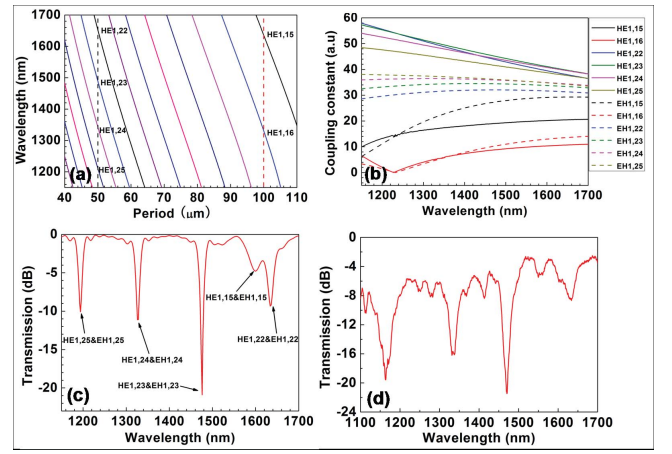


Fig. 2. (a) Relationship of the grating period and the resonant wavelength of different high-order cladding modes (HE1,15 and HE1,16 correspond to the first-order diffraction, HE1,22 ~ HE1,25 correspond to the second-order diffraction). (b) Coupling constants of different high-order cladding modes with the wavelength range of 1200 ~ 1700 nm. (c) Theoretically simulated transmission spectrum. (d) Typical transmission spectrum of the LPFG with a period of 100 μ m.

the coupling strength of the HE1,16 mode to the guided mode is so weak that the coupling can be neglected at the resonant wavelength of 1330 nm, and only a weak coupling occurs at the resonant wavelength of 1635 nm, which belongs to the HE1,15 mode. On the contrary, the coupling strengths of the second-order diffraction are all strong enough to generate deep loss peaks in the transmission spectrum. The higher-order EH modes of second-order diffraction exhibit strong coupling strengths close to the HE modes. Fig. 2(c) shows the calculated transmission spectrum, which agrees well with the experimental result in Fig. 2(d).

IV. SENSING CHARACTERISTICS

The loss peak around 1470 nm corresponding to the HE1,23 mode at the second-order diffraction was chosen for sensing applications. The LPFG was first placed in a digitally controlled muffle furnace, where it was gradually heated up to 800 $^{\circ}$ C and kept for 2 hours. It was then cooled down to the room temperature (20 $^{\circ}$ C). No obvious degradation in the strength of the grating was found after this pre-annealing process, which was generally used for erasing the so-called Type-I IR grating that features temperature-unstable structure [15]. Later, the furnace was first heated up from the room temperature to 100 $^{\circ}$ C, and then to 700 $^{\circ}$ C with the increment of 100 $^{\circ}$ C for one step. After one-step increment, the grating was kept at that temperature for 30 minutes and the transmission spectrum was recorded at each step. It is found that as the temperature increases, the wavelength of the chosen loss peak has a blueshift as shown in Fig. 3. The temperature sensitivity is obtained as low as -15.52 pm/ $^{\circ}$ C from a linear fit in the range of 20 $^{\circ}$ C ~ 500 $^{\circ}$ C, which is of the same magnitude as that of the FBGs [11], but 6 times smaller than that of the LPFGs [10]. In the temperature range of 500 $^{\circ}$ C ~ 700 $^{\circ}$ C, the sensitivity becomes -37 pm/ $^{\circ}$ C. The nonlinear shift of the resonant wavelength may be caused by thermal and mechanical stress development in the fiber

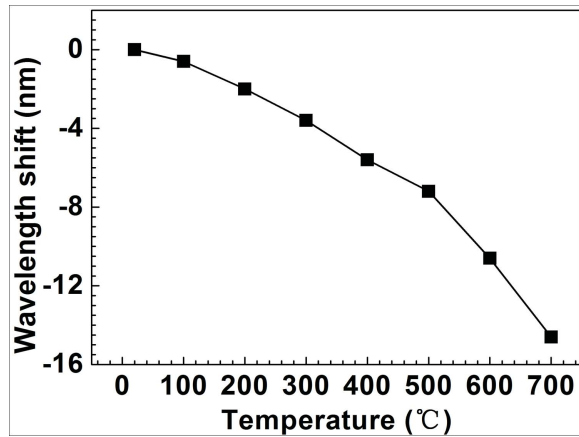


Fig. 3. Shift of the loss peak wavelength of the LPFG with temperature.

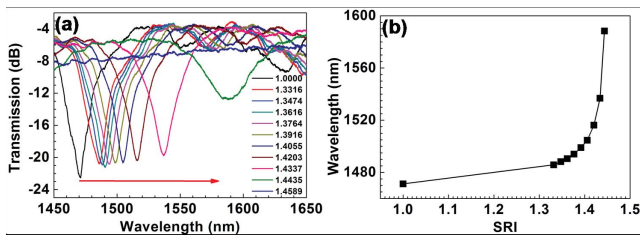


Fig. 4. (a) Transmission spectra of LPFG with different RI solutions. (b) Shift of the loss peak wavelength of the LPFG with different RI solutions.

at high temperatures [16]. The small temperature coefficient is desired for applications in which cross-talk resulting from multiple-parameter sensing effects needs to be avoided.

We also measured the RI sensitivity of the LPFG. The fiber grating was placed into a hard plastic slot and kept straight in the entire course of measurement to prevent from bend-induced spectral changes. After the LPFG was fixed, we injected RI solutions into the plastic slot so that the LPFG was totally immersed. After the spectrum was recorded, the LPFG was then cleaned with ethanol and pure water, and dried by compressed air. The procedure was repeated to measure the other RI solutions (different volume ratio of glycerin and water mixed solutions). The RI of the solution was calibrated by an Abbe refractometer. The loss peak around 1470 nm was once again selected. It is found that a redshift of 120 nm was obtained as RI increases from 1.0 to 1.443, as shown in Fig. 4. The shift becomes faster when the RI is close to the effective RI of the cladding mode. Starting from RI of 1.443, the loss peak becomes weaker and weaker as RI increases and finally disappears when $RI = 1.458$. The RI sensitivity of the compact 100- μm LPFGs is found to be higher than the ordinary period LPFGs ($\sim 500 \mu\text{m}$) due to the coupling of the guided mode to the extremely higher forward-propagating cladding modes. The average sensitivities of this peak in the RI range of 1.332 \sim 1.391 and 1.391 \sim 1.433 are about 216 nm/RIU (RI unit) and 883 nm/RIU, respectively. Surprisingly, the sensitivity reaches as high as 5265 nm/RIU in the RI range of 1.433 \sim 1.443.

V. CONCLUSION

In conclusion, compact 100- μm -period LPFGs with 5-mm grating-bearing region were fabricated by femtosecond laser direct writing. The photomodified grating segments were located at the center of the fiber core with no damage to the cladding. The resonant loss peaks of the LPFGs from the coupling between the guided mode and the high-order cladding modes occur, which were found to possess higher sensitivity to the RI variation. Particularly the coupling of the $HE_{1,22} \sim HE_{1,25}$ modes to the guided mode at the second-order diffraction was experimentally verified. The transmission spectra of the LPFG exhibit blueshift as temperature increases, but redshift as RI increases. A very high RI sensitivity of 5265 nm/RIU in the RI range of 1.433 \sim 1.443 and a low temperature sensitivity of only $-15.52 \text{ pm}/^\circ\text{C}$ from 20 $^\circ\text{C}$ to 500 $^\circ\text{C}$ have been achieved, making these LPFGs good candidates for RI sensors to reduce the cross-talk sensitivity from temperature variation.

REFERENCES

- [1] A. M. Vengsarkar, P. J. Lemaire, J. B. Judkins, V. Bhatia, T. E. Ergodan, and J. E. Sipe, "Long-period fiber gratings as band-rejection filters," *J. Lightw. Technol.*, vol. 14, no. 1, pp. 58–65, Jan. 1996.
- [2] V. Bhatia and A. M. Vengsarkar, "Optical fiber long-period grating sensors," *Opt. Lett.*, vol. 21, no. 9, pp. 692–694, May 1996.
- [3] H. J. Patrick, C. C. Chang, and S. T. Vohra, "Long period fibre gratings for structural bend sensing," *Electron. Lett.*, vol. 34, no. 18, pp. 1773–1774, Sep. 1998.
- [4] B. H. Lee, Y. Liu, S. B. Lee, S. S. Choi, and J. N. Jang, "Displacements of the resonant peaks of a long-period fiber grating induced by a change of ambient refractive index," *Opt. Lett.*, vol. 22, no. 23, pp. 1769–1772, Dec. 1997.
- [5] H. J. Patrick, A. D. Kersey, and F. Bucholtz, "Analysis of the response of long period fiber gratings to external index of refraction," *J. Lightw. Technol.*, vol. 16, no. 9, pp. 1606–1612, Sep. 1998.
- [6] X. W. Shu, X. M. Zhu, Q. L. Wang, S. Jiang, W. Shi, Z. J. Huang, and D. X. Huang, "Dual resonant peaks of LP015 cladding mode in long-period gratings," *Electron. Lett.*, vol. 35, no. 8, pp. 649–650, Apr. 1999.
- [7] S. R. Baker, H. N. Rourke, V. Baker, and D. Goodchild, "Thermal decay of fiber Bragg gratings written in boron and germanium codoped silica fiber," *J. Lightw. Technol.*, vol. 15, no. 8, pp. 1470–1477, Aug. 1997.
- [8] R. R. Gattass and E. Mazur, "Femtosecond laser micromachining in transparent materials," *Nat. Photon.*, vol. 2, pp. 219–225, Apr. 2008.
- [9] Y. L. Zhang, Q. D. Chen, H. Xia, and H. B. Sun, "Designable 3D nanofabrication by femtosecond laser direct writing," *Nano Today*, vol. 5, no. 5, pp. 435–448, Dec. 2010.
- [10] Y. Kondo, K. Nouchi, T. Mitsuyu, M. Watanabe, P. G. Kazansky, and K. Hirao, "Fabrication of long-period fiber gratings by focused irradiation of infrared femtosecond laser pulses," *Opt. Lett.*, vol. 24, no. 10, pp. 646–648, May 1999.
- [11] C. Chen, Y. S. Yu, R. Yang, L. Wang, J. C. Guo, Q. D. Chen, and H. B. Sun, "Monitoring thermal effect in femtosecond laser interaction with glass by fiber Bragg grating," *J. Lightw. Technol.*, vol. 29, no. 14, pp. 2126–2130, Jul. 15, 2011.
- [12] L. Wang, *et al.*, "Maskless laser tailoring of conical pillar arrays for antireflective biomimetic surfaces," *Opt. Lett.*, vol. 36, no. 17, pp. 3305–3307, Sep. 2011.
- [13] T. Erdogan, "Cladding-mode resonances in short- and long-period fiber grating filters," *J. Opt. Soc. Amer. A*, vol. 14, no. 8, pp. 1760–1773, Aug. 1997.
- [14] X. W. Shu, L. Zhang, and I. Bennion, "Fabrication and characterisation of ultralong period fibre gratings," *Opt. Commun.*, vol. 203, pp. 277–281, Mar. 2002.
- [15] C. W. Smelser, S. J. Mihailov, and D. Grobnc, "Formation of Type I-IR and Type II-IR gratings with an ultrafast IR laser and a phase mask," *Opt. Express*, vol. 13, pp. 5377–5386, Jul. 2005.
- [16] G. Humbert and A. Malki, "Characterizations at very high temperature of electricarc-induced long-period fiber gratings," *Opt. Commun.*, vol. 208, pp. 329–335, Jul. 2002.